

Photochemistry of adsorbed molecules. V. Ultraviolet photodissociation of OCS on LiF(001)

K. Leggett, J. C. Polanyi, and P. A. Young

Citation: *The Journal of Chemical Physics* **93**, 3645 (1990); doi: 10.1063/1.458795

View online: <http://dx.doi.org/10.1063/1.458795>

View Table of Contents: <http://scitation.aip.org/content/aip/journal/jcp/93/5?ver=pdfcov>

Published by the [AIP Publishing](#)

Articles you may be interested in

Photochemistry of adsorbed molecules. IX. Ultraviolet photodissociation and photoreaction of HBr on LiF(001)
J. Chem. Phys. **95**, 1361 (1991); 10.1063/1.461118

Photochemistry of adsorbed molecules. VII. Ultraviolet photoejection and photodesorption of OCS on LiF(001)
J. Chem. Phys. **93**, 3673 (1990); 10.1063/1.458797

Photochemistry of adsorbed molecules. VI. Ultraviolet photoreaction of OCS on LiF(001)
J. Chem. Phys. **93**, 3659 (1990); 10.1063/1.458796

Photochemistry of adsorbed molecules. IV. Photodissociation, photoreaction, photoejection, and photodesorption of H₂S on LiF(001)
J. Chem. Phys. **89**, 1498 (1988); 10.1063/1.455716

Photochemistry of adsorbed molecules. III. Photodissociation and photodesorption of CH₃Br adsorbed on LiF(001)
J. Chem. Phys. **89**, 1475 (1988); 10.1063/1.455148



Photochemistry of adsorbed molecules. V. Ultraviolet photodissociation of OCS on LiF(001)

K. Leggett,^{a)} J. C. Polanyi, and P. A. Young^{b)}

Department of Chemistry, University of Toronto, Toronto M5S 1A1, Canada

(Received 4 August 1989; accepted 2 May 1990)

Dynamical studies of the UV photochemistry of submonolayer coverages of OCS physisorbed on 116 K LiF(001) are presented. Following pulsed ultraviolet laser irradiation (λ 222 nm), translational energy and angular distributions were obtained for photolysis products by angle-resolved time-of-flight mass spectrometry. Photolysis of adsorbates gave rise to distributions which differed markedly from gas phase photodissociation. Energetic sulphur and CO fragments were detected for coverages $\geq 10^{-5}$ monolayers. The cross section for photolysis in the adsorbed state was enhanced 10^3 – $10^4 \times$ relative to the gas phase. The dynamics for these photoprocesses were found to vary with adsorbate coverage, indicative of a catalytic influence of the surface on the photochemistry.

I. INTRODUCTION

The possibility of inducing photochemical processes within adsorbed layers by laser irradiation has attracted substantial attention in recent years.¹ This interest is motivated both by the scientific importance and by potential applications to novel-materials fabrication and microelectronics.

The scientific interest arises, in part, from the observation that certain photochemical processes in adsorbed molecules may be substantially altered relative to the corresponding process in the gas phase. An example in the realm of spectroscopy is surface-enhanced Raman scattering (SERS). Adsorption of molecules on a variety of roughened metal surfaces is found to lead to Raman scattering cross sections many orders-of-magnitude (ca. 10^5 – $10^6 \times$) larger than those found in the gas phase.²

In the present work, a new class of surface-enhanced process, namely surface-enhanced photodissociation, is reported. A preliminary account of this phenomenon has already appeared;³ a more detailed study is described here. At low coverages ($\sim 10^{-4}$ monolayers), cross sections for OCS photodissociation at 222 nm are found to be enhanced $\sim 10^3$ – $10^4 \times$ relative to the gas phase, and are shown to depend on adsorption site. We propose that the mechanism involves efficient long range electronic energy transfer from defect centers in the crystal to the adsorbed OCS. This, and other, mechanisms are discussed below.

This paper reports dynamical studies of photochemistry of the linear triatomic OCS physisorbed on single crystal LiF.⁴ Energetic sulphur and CO fragments were observed in good yield under 222 nm irradiation and ascribed to the surface-aligned photodissociation (SAPDIS, abbreviated to PDIS) of OCS(*ad*). The sulphur photofragment angular distribution peaked around the surface normal, believed to reflect the range of preferred molecular orientations on LiF(001) at 115 K. The S and CO photofragment translational energy distributions were consistent with a

major alteration in the dissociation dynamics as compared with the gas phase. Possible origins of the dynamical changes will be discussed.

In two companion publications following the present work, the photochemical channels of surface-aligned photoreaction (PRXN),⁵ photoejection (PEJ) and photodesorption (PDES)⁶ of OCS(*ad*) on LiF(001) will be described. In particular, PDIS and PRXN are strongly correlated, since the atomic sulphur formed in PDIS serves as a reagent for PRXN.

Ultraviolet (UV) photodissociation of adsorbates has been reported for an increasing number of systems. Early studies performed at substantial gas pressures above the surface gave persuasive, though indirect, evidence for the UV photodissociation of adsorbates.^{7,8} Since then, photochemistry has been studied in high vacuum using time-of-flight (TOF) mass spectrometry to detect photofragments ejected from submonolayers of adsorbates on single crystals of alkali halides,^{9–13} multilayer adsorbates and polycrystalline ices.^{14–19} In addition, photolysis of adsorbates has been followed by x-ray photoelectron spectroscopy on dielectric substrates^{17,18} and metals,^{17,19} as well as by Auger electron spectroscopy on semiconductors²⁰ and metals.²¹

Bourdon *et al.*^{9,10} and Harrison *et al.*,^{11,12} working in this laboratory, used TOF mass spectrometry for dynamical studies of adsorbate photochemistry on a LiF(001) substrate under ultrahigh vacuum (UHV) conditions. In studies of CH₃Br(*ad*) photodissociation at 222 nm, the methyl radical translational energy distribution was found to differ from that in the gas phase; it was sensitive to adsorbate phase and to substrate heat treatment. Substantial yields of energetic bromine atoms were detected with translational energies in excess of that observed in the gas phase photodissociation. These energetic atoms were at-

^{a)}Present address: Department of Chemistry, University of Pennsylvania, Philadelphia, Pennsylvania 19104.

^{b)}Present address: Ontario Centre for Materials Research, Interface Science and Technology, University of Western Ontario, London N6A 5B7, Ontario.

tributed to secondary encounters between recoiling Br and CH₃ fragments chattering to and fro between the Br and the LiF surface.^{10,11}

Photodissociation of adsorbed H₂S at 222 and 193 nm produced energetic atomic H fragments with a bimodal translational energy distribution, corresponding to recoil from either HS($\nu=0$) or HS[†]($\nu\approx 2$). The photolytic branching ratio HS[†]/HS from adsorbed H₂S was enhanced relative to the gas phase value and was a sensitive function of adsorption site.^{10,12}

Tabares *et al.*¹³ studied the 193 nm photochemistry of CH₃Br on LiF(001) in a lower temperature regime (30–90 K). The translational energy distributions they observed using TOF mass spectrometry were substantially broader and shifted to lower energy as compared with those obtained by Bourdon *et al.* and Harrison *et al.*^{10,11} on 115 K LiF(001). The lower surface temperatures in the Tabares study were thought to result in formation of three dimensional clusters of adsorbate. Dissociation occurred throughout the cluster; hence photofragments formed within the deposit suffered multiple collisions prior to scattering into the detector. This would account for the more relaxed appearance of the photofragment energy distributions in the Tabares experiments.

Nishi *et al.*¹⁴ studied the photochemistry of NH₃ and H₂O ices. Both single and multiphoton dissociation fragments were detected using TOF mass spectrometry. Photolysis products were also detected from actinic impurities in doped CO₂ crystals.¹⁵ Very recently, Kutzner and co-workers¹⁶ used multiphoton ionization (REMPI) to study the 266 nm photodissociation of polycrystalline CH₃I(*ad*) on LiF. Formation of both I and I* could be distinguished in the velocity distribution of the CH₃ fragments.

Evidence is also found for UV photodissociation of adsorbed molecules on more chemically active semiconductor²⁰ and metallic substrates.^{17–19,21} Photolysis of adsorbed (CH₃)₃Al on Al₂O₃, SiO₂ or Si/SiO₂ substrates²² produced methyl fragments characterized by low translational energies (equivalent temperatures ~ 150 K). This was attributed to a long-lived excited state complex which dissipated much of the original excitation energy to the substrate. Using TOF techniques, Domen and Chuang^{17,19} found dissociation of CH₂I₂ on Ag surfaces for coverages greater than 1 ML produced CH₂I fragments with peak translational energies ~ 0.12 eV.

Harrison and Polanyi²³ assessed the feasibility of performing crossed molecular beam experiments employing laser irradiated adsorbates as sources. The ablated material could be formed by any of laser photodissociation, photoejection or thermal desorption.

The present study makes use of an adsorbate, OCS, whose UV absorption spectrum has been extensively studied in the gas phase. The $A^1\Delta \leftarrow X^1\Sigma^+$ system near 2237 Å is a broad, structureless continuum and corresponds to a $\pi^* \leftarrow \pi$ excitation.^{24–26} This transition is not as strongly forbidden as is normally the case for a quadrupole allowed transition of $^1\Delta \leftarrow ^1\Sigma^+$ symmetry ($f = 1.8 \times 10^{-3}$);²⁴ OCS bending renders these symmetry labels approximate.

The OCS gas phase absorption cross section at 222 nm is 1.1×10^{-19} cm² per molecule.²⁷

The first suggestions that photolysis of carbonyl sulphide in the $A \leftarrow X$ band resulted in CO and excited state S* (= S(¹D)) appeared over fifty years ago.²⁸ Studies of the trapping products gave a gas phase photolytic branching ratio $R = (S^*/S)$ of $\sim 0.75/0.25$, although this value was controversial.²⁹ In liquid phase photolysis, excited state S* was also formed, but with lower relative yield. This was attributed to more efficient relaxation of the S* to the ground state in the condensed phase or to an intersystem crossing correlating with ground state sulphur. Irradiation of solid OCS/propylene at liquid nitrogen temperature was also found to produce S*, but with diminished yield.²⁵

Joens and Bair³⁰ evaluated the extent of CO vibrational excitation in the 222 nm flash photolysis of OCS(*g*) and determined that for the primary photolysis, the average state in CO was $\nu < 0.25$.

The 222 nm photodissociation dynamics of *gas phase* OCS have been thoroughly studied by Sivakumar *et al.*³¹ Using laser induced fluorescence (LIF), the state distribution of both the sulphur and CO fragments were measured. Photodissociation of OCS(*g*) at 222 nm led to only S*; the quantum yield of ground state S was ≤ 0.02 . The photolytic CO was produced entirely in $\nu=0$; it populated two overlapping rotational distributions centered, respectively, around $J=55$ and 66. The gas phase translational energy distributions can, therefore, be deduced from momentum and energy conservation for comparison with the distributions from photolysis in the adsorbed state, as reported in this paper.

The two “peaks” in the CO rotational distribution arise in the gas phase from dissociation through two components of the ¹Δ state. As the symmetry of the molecule in the excited state is reduced from C_{∞v} (linear) to C_s (bent), the ¹Δ state splits into ¹A' and ¹A'' components. The relative contributions from the ¹A' and ¹A'' states determine the product CO rotational state.³¹ Dissociation leading to CO (high J) occurs principally through the ¹A' state. Further, the angular distribution of the CO (high J) is sharply peaked along the laser polarization direction. Hence, the moment for the A' transition is parallel to the C–S bond, while for the A'' transition, the moment is perpendicular to the plane of the OCS molecule.

The 222 nm photolysis of OCS(*ad*) on LiF(001) producing energetic sulphur and CO fragments is described in this paper. In the following paper, we report the surface-aligned photoreaction (PRXN) of the atomic sulphur photofragment with co-adsorbed OCS(*ad*) to produce S₂. Reaction occurs in good yield. Two distinct reaction dynamics are evidenced in the S₂ translational energy distribution.^{4,5} The observed changes in the PRXN translational energy distribution with increased coverage are likely to reflect an altered reagent alignment in multilayer OCS films.^{4,5}

II. EXPERIMENT

The surface photochemistry apparatus has been previously described in detail.^{4,10,11} The ultrahigh vacuum

(UHV) apparatus was equipped for cleaning and characterization of the crystals and operated at a base pressure of $\sim 6 \times 10^{-11}$ Torr. Single crystal LiF was obtained from the Harshaw Chemical Co., cleaved in air and mounted in vacuum on a homebuilt LN₂ cooled target manipulator. Surface temperature measurement was by means of a chromel–alumel thermocouple embedded in the crystal.

Under operating conditions the crystal was held at 116 K. The surface was dosed continuously with adsorbate by means of directed or background sources. Adsorbate coverages were maintained in equilibrium between the dosing and efficient removal of adsorbate molecules by several photochemical processes. Experiments were conducted over a range of dosing from $\sim 10^{-5}$ to 37 L (where 1 L = 10^{-6} Torr s). Both the sticking probability S and removal efficiency ϵ were close to unity for a wide range of doses and laser pulse energies. Hence, the estimated OCS(ad) coverages ranged from $\sim 10^{-5}$ ML to several monolayers.

Photoproduct detection was by means of a doubly differentially pumped quadrupole mass spectrometer. The crystal to ionizer distance was 23.6 cm. The chemical identity and corresponding translational energy distributions were obtained from the mass selected TOF spectra. Only positive ion signals were examined in these experiments. Signal averaging of typically 10^2 – 10^4 laser pulses duration was performed on-line by computer.

The wavelengths employed in this study were 222 and 308 nm (KrCl and XeCl excimers, respectively) with energies ranging from ~ 0.5 – 15 mJ/laser pulse. The excimer laser irradiated a 0.3 cm² area of the crystal at glancing incidence. Product angular distributions, $P(\theta)$, were obtained by rotating the crystal about the laser beam axis. The illumination of the target remained constant while the surface polar angle θ with respect to the (fixed) detector varied. Laser repetition rates varied from 1–20 Hz.

Experiments were performed on both annealed (700 K for 12 h in UHV) and unannealed (450 K for 8–12 h in UHV) LiF crystals. It is believed that this annealing treatment leads to the preparation of a well ordered LiF(001) face by evaporation of surface excess Li metal and annealing of surface point defects.³² Hence, the principal distinction between annealed and unannealed LiF arose solely from differences in the numbers and types of surface defect sites. Unannealed LiF(001) was expected to possess a greater number and diversity of surface defect sites than annealed LiF(001). The characteristics of these defect sites were not studied in the present work.

Carbonyl sulphide (purity >97.7 mole%) was obtained from Matheson Gas Products. The major impurities were reported as CO₂ (1.4 mole%), CO/N₂ (0.6%) and CS₂ (0.19%).³³ Of these impurities, only CS₂ has an appreciable 222 nm gas phase absorption cross section σ_{ab} : $\sim 1 \times 10^{-20}$ cm² per molecule ($\sim 10\%$ that of OCS at 222 nm).²⁴ Thus, the fractional contribution to the atomic sulphur photo-fragment yield expected from CS₂ dissociation would be $\sim 10^{-4} \times$ the OCS yield.

Reported adsorbate doses were corrected for the ion gauge sensitivity S of OCS relative to thermal N₂, as esti-

mated by the Dushman formula:³⁴ $S_{\text{OCS}}/S_{\text{N}_2} = 1.61$. As the operating parameters of the mass spectrometer ionizer (incident electron energy 100 eV) and a typical nude ionization gauge (incident electron energy ~ 150 eV) were similar, these estimated sensitivities were taken to give a satisfactory measure of the ionization efficiency in the mass spectrometer. Hence, photofragment yields were quantitatively determined using the corresponding gauge sensitivity; for sulphur atoms $S_{\text{S}} = 1.07$ while for CO molecules, $S_{\text{CO}} = 1$.

Visual examination of the LiF crystals after exposures to adsorbate + laser of $\sim 10^7$ laser pulses showed evidence of slight darkening. Auger spectra taken of these “typical” crystals showed a depletion of fluorine relative to a freshly cleaved crystal and trace sulphur deposition. The fluorine depletion increased with successive Auger measurements; we believe the incident electron beam was responsible. Quantitative determination of the concentration of sulphur deposit was precluded due to the unstable Auger intensities.³⁵ The likely origin of this deposit must have been some low probability UV initiated adsorption process, possibly originating from a restricted precursor geometry.

The observed photodissociation described here is not a consequence of this deposit, as photolysis could be observed for the first laser shots on freshly prepared crystals. To minimize the possible contribution of any accumulating surface deposit, crystals were routinely replaced after about 10^7 laser pulses. Attempts to thermally evaporate the deposit were unsuccessful, being restricted, by necessity, to ≤ 870 K at which temperature the LiF softens.³⁶

Temperature programmed desorption (TPD) was employed to provide complementary information on the adsorbate-surface bond energy and the sticking probability S . The adsorption energy was coverage dependent and ranged from ca. 0.38 eV (0.03L) reaching 0.28 eV in the region of 1 monolayer. Only a single peak was observed in TPD; desorption temperatures ranged from 134 to 124 K. It is noteworthy that this latter value is in agreement to the bulk heat of sublimation for OCS(s) (0.28 eV).³⁷ The sticking probability S was estimated as unity for OCS(ad) doses ≤ 4 L. A monolayer of OCS(ad) was taken to comprise 6.5×10^{14} molecules per cm².³⁸

III. RESULTS AND DISCUSSION

In the course of these experiments both atomic sulphur and molecular CO photofragments were examined. Evidence from the photodissociation angular distributions at low coverages suggest that the molecules are adsorbed vertically (see below). The detected energetic fragments discussed in the following sections were thought to arise from photodissociation of molecules for which the photofragment was initially directed away from the surface. For photofragments directed toward the surface, collision with the surface would be likely to produce photofragments with a broad angular distribution,³⁹ rather than the observed $\cos \theta$ distribution. Detection of these scattered photoproducts and discrimination from background signals would be less likely than that of species that do not undergo surface scattering.

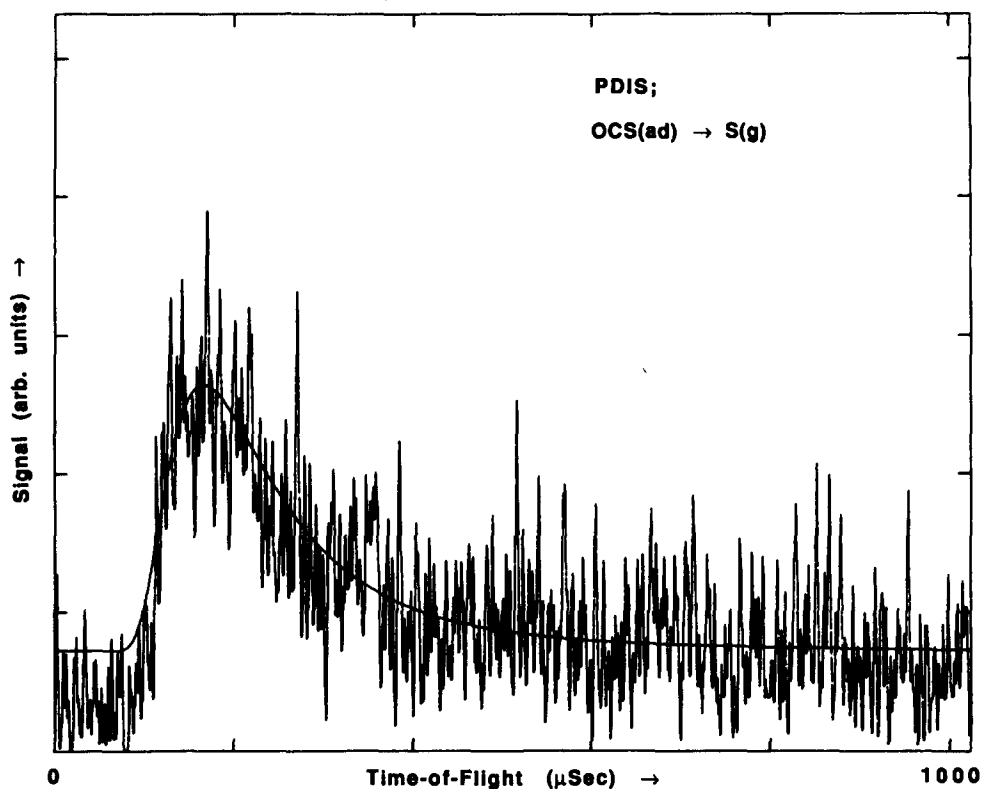


FIG. 1. Time-of-flight spectrum of atomic sulphur photofragment from the 222 nm photodissociation (PDIS) of OCS physisorbed on annealed LiF(001) at 116 K. The OCS(*ad*) dose was 1.2×10^{-3} L, with a laser energy of 8.4 mJ/laser pulse and a detection angle of 5° with respect to the surface normal. For these conditions, it was estimated that the surface coverage was equal to the dose; that is 1.2×10^{-3} ML (monolayer = ML). The spectrum represents the average of 6000 laser pulses. The smooth curve is the least squares fit to the experimental data. Under the conditions of the experiment, the yield of slow-moving molecular photodesorption, (PDES), is negligible (see text).

A. Sulphur photofragment

Figure 1 shows a time-of-flight (TOF) spectrum for the sulphur photofragment from the 222 nm photodissociation of OCS physisorbed on annealed LiF(001). The smooth curve through the experimental data represents the nonlinear least squares fit to a Maxwellian velocity distribution with a superimposed stream velocity.^{11,12} This fitted TOF was transformed to give the translational energy distribution $P(T')$ shown in a subsequent figure.

The total flux of photodissociation products (both S and CO), integrated over the hemisphere above the illuminated area of the crystal was determined to be 4.4×10^{10} particles at the stated wavelength, energy and coverage of Fig. 1.

A detailed calculation relating the number of photofragments observed, the adsorbate coverage and the effective laser intensity at the surface to the apparent photolytic cross section in the adsorbed state, indicated a dramatic departure from gas phase dissociation dynamics. The 222 nm cross section in the adsorbed state, $\sigma_{ph}(ad)$, was found to be $\sim 1-10 \text{ \AA}^2/\text{mol}$,³ as compared with a gas phase $\sigma_{ph}(g)$ of $\sim 0.001 \text{ \AA}^2/\text{mol}$.²⁷ The enhancement decreased monotonically with increasing adsorbate dose. The dependence of the photolytic cross section enhancement on the OCS(*ad*) dose on unannealed LiF(001) at 116 K is illustrated in Fig. 2. As the enhancement in $\sigma_{ph}(ad)$ was a decreasing function of coverage, this suggested that the enhancement effect originated from a limited set of active adsorption sites on the surface. The possible mechanisms leading to an enhanced photolytic cross section are discussed in greater detail in Sec. D.

The photolysis yield as a function of laser energy was not measured, since under the experimental conditions the

adsorbate coverage and laser pulse energy were not independent. However, the S photofragment energy distribution was consistent with a single photon photodissociation. Under the focussing conditions employed here, these laser

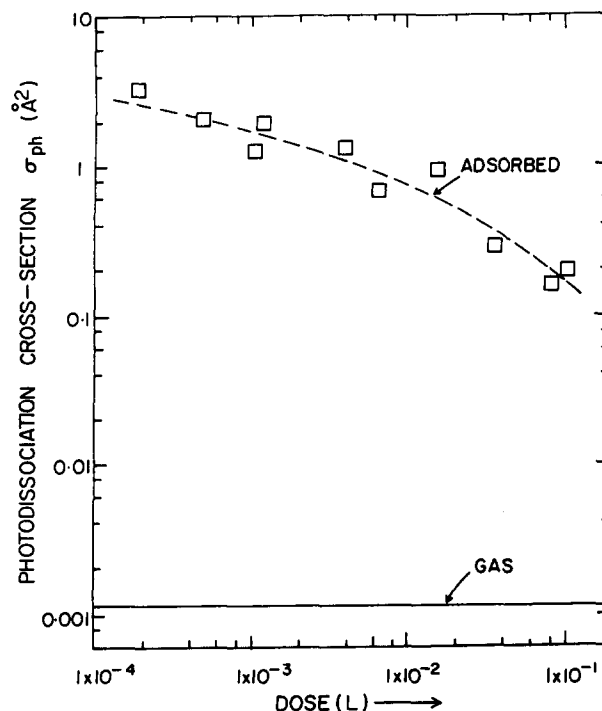


FIG. 2. The dependence of the adsorbed state photodissociation cross section $\sigma_{ph}(ad)$ at 222 nm on OCS dose for unannealed LiF(001). The gas phase cross section at 222 nm (0.0011 \AA^2 per molecule) is presented for comparison.

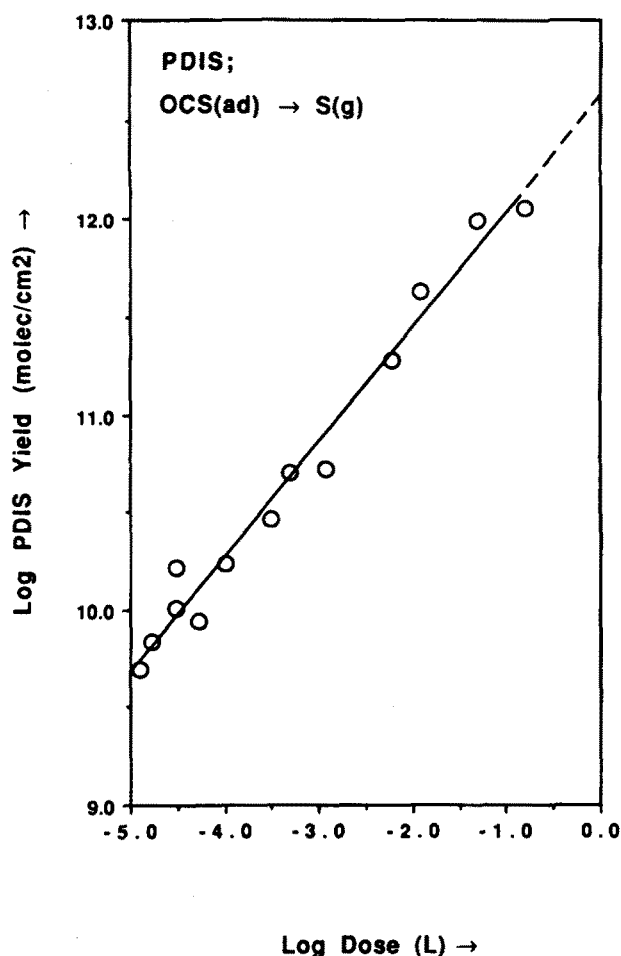


FIG. 3. Atomic sulphur photofragment yield as a function of OCS dose for the 222 nm PDIS of physisorbed OCS. The substrate was annealed LiF(001) at 116 K. The yields were normalized to a constant laser energy. The solid line through the points represents the linear least squares fit to the data.

powers of $\leq 4.5 \text{ MW/cm}^2$ were unlikely to initiate multi-photon UV processes.⁴⁰

Figure 3 illustrates the dependence of the yield of S photofragments on the adsorbate dose. The photolysis yield increased proportional to the square root of the adsorbate dose over the range of 1×10^{-5} to 0.17 L/laser pulse (OCS(ad) coverages from 10^{-5} to $\sim 0.2 \text{ ML}$). For submonolayer coverages one would expect the yield to increase linearly with coverage. However, the decreasing cross section enhancement with increasing coverage will give a smaller net rate of increase.

For coverages greater than 0.2 ML, yields of photofragments could only be estimated, as photolysis products were partially obscured in time-of-flight by the efficient molecular photodesorption (PDES) channel; see Fig. 4. The low photofragment translational energy resulted in poor TOF separation between photofragments and molecular photodesorbates. No reliable deconvolution of the PDIS signal from the $\sim 100 \times$ larger PDES signal could be obtained in the coverage range $\geq 0.2 \text{ ML}$.

The sulphur photofragment translational energy distributions, $P(T')$, distributions depended slightly on the crystal surface. Unannealed LiF(001) was found to give a somewhat less energetic distribution with a peak translational energy, T'_p , of 0.18 eV (cf. T'_p for annealed LiF(001) of 0.24 eV). By contrast, in previous work the methyl radical peak energy T'_p from the 222 nm photodissociation of $\text{CH}_3\text{Br(ad)}$ was found to decrease by $\sim 1.4 \text{ eV}$ upon changing the substrate from annealed to unannealed LiF(001).¹¹ In the present instance, the effect of crystal annealing is likely to be less dramatic since $P(T')$ already peaks at a low T' .

Figure 5 (a) gives the atomic sulphur fragment translational energy distribution $P(T')$ from the 222 nm pho-

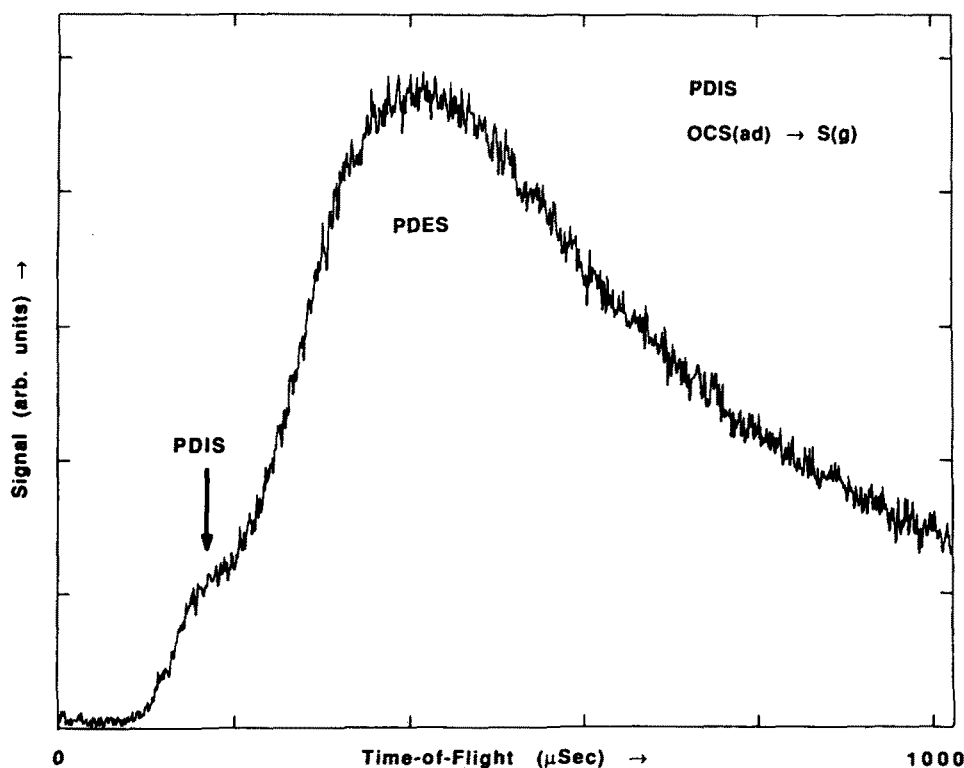


FIG. 4. Time-of-flight spectrum of sulphur photofragment from the 222 nm PDIS and PDES of OCS adsorbed on annealed LiF(001). The OCS dose was 0.17 L/laser pulse, detection angle 5° and laser energy of 9 mJ/laser pulse. The surface coverage was estimated to be 0.2 ML. The vertical arrow locates the PDIS peak from Fig. 1. At this coverage, the PDIS channel is substantially overlapped in time-of-flight by the dominant PDES channel, making deconvolution difficult.

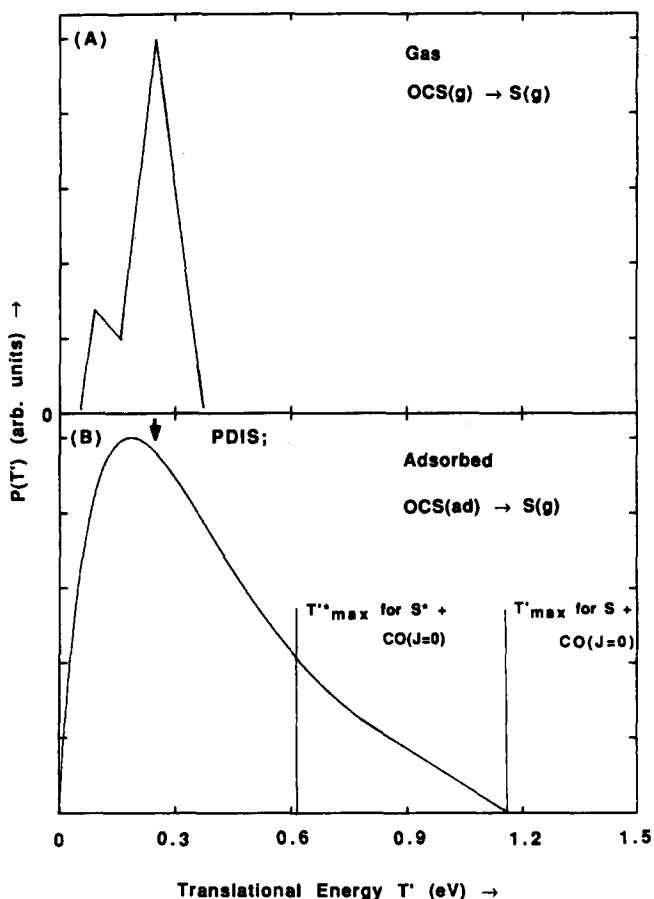


FIG. 5. Translational energy distribution $P(T')$ for the sulphur fragment from the 222 nm photodissociation of OCS. (a) Gas phase distribution as inferred from the measured product state distribution of Sivakumar *et al.* (Ref. 31) (bimodal structure reflects the population of two rotational components of the CO fragment energy distribution). (b) Adsorbed phase distribution as determined from the TOF spectrum of Fig. 1. The vertical arrow marks the peak of the gas phase translational energy distribution. The maximum "thermodynamic" translational energies for formation of ground and excited state atomic sulphur are also shown.

photodissociation of *gaseous* carbonyl sulphide as reported from another laboratory.³¹ This distribution was inferred from the measured state distributions of the S and CO fragments in laser induced fluorescence (LiF) experiments. The "sawtooth" pattern in the translational energy distribution reflects the production of the CO fragment in two rotational distributions, peaked at $J=55$ and 66 , respectively. Only S^* was produced, as the yield of ground state S was below the detection limit (quantum yield ≤ 0.02).³¹

Figure 5(b) is the corresponding sulphur translational energy distribution $P(T')$ obtained for OCS physisorbed on annealed LiF(001). This is the energy distribution corresponding to the TOF shown in Fig. 1. The peak translational energy, T'_p , was 0.18 eV and FWHM (abbreviated T'_{FW}) was 0.51 eV. The dramatic differences between the gas phase and adsorbed phase $P(T')$ distributions will now be discussed.

First, there is no evidence of bimodality in the translational energy distribution of S from adsorbate photolysis, in spite of an energy resolution sufficient in the present

work to resolve the bimodality in the gas phase photolysis. The peak translational energies for photofragments originating from gas and "surface" photolysis were similar: $T'_p = 0.24$ eV (average for annealed LiF, over our range of coverages) versus 0.27 eV for the gas.

For OCS(*ad*) photolysis, 50% of the sulphur photo-products had translational energies in excess of the maximum T' observed in the gas phase, and a total of 25% of the product had T' in excess of T'^* allowed for dissociation products correlated with excited state S^* and CO($J=0$). This implies a major alteration in the branching ratio between S^* and S from all S^* in the gas phase to a ratio $R = (S^*/S) = 3$ in the adsorbed state. This ratio was calculated assuming that all sulphur fragments with translational energies in excess of the T'^* correlating with S^* and CO($J=0$) were ground state S atoms, and the remainder constituted *solely* S^* atoms. The relative yield of ground state S atoms may well be underestimated, since for CO($J>0$) atomic S product will have $T' < T'^*$. It follows that the S^*/S value of 3 in the adsorbed state is an upper limit.

In the gas phase the bimodality in the translational energy distribution $P(T')$ was attributed to the parallel and perpendicular transitions to the $^1A'$ and $^1\Delta$ states, respectively. The altered $P(T')$ observed for OCS(*ad*) could not be obtained from any superposition of these two gas phase components. The polarization of the laser radiation at the surface varies with detection angle; see Refs. 4 and 11. In the adsorbed state, no variation in PDIS translational energy distribution was observed with detection angle, evidence for a lack of a specific $P(T')$ for parallel or perpendicular transitions.

Since our crystal temperature is at the measured thermal desorption temperature for CO on LiF(001), i.e. 116 K, photofragment CO recoiling from OCS in PDIS is unlikely to be adsorbed.

Figure 6 presents the variation in translational energy distribution peak and breadth with OCS(*ad*) dose for the sulphur photofragment. The peak energy, T'_p , increased from ~ 0.13 to 0.18 eV, while the FWHM increased from ~ 0.38 to 0.44 eV over a range of coverages 10^{-4} to 0.1 ML. We find that for OCS the heat of adsorption decreases with increasing coverage. The small increases in T'_p and T'_{FW} for the photolytic sulphur could be linked to the lessened coupling of the CO "end" of the OCS molecule to the LiF surface at higher coverages.

This sensitivity to surface forces is consistent with the observation that the cross section for photodissociation, $\sigma_{ph}(ad)$, and the PDIS energy distributions are substantially altered as compared with gas phase dissociation dynamics.

In understanding the partitioning of product translational motion and CO internal excitation, it is noteworthy that photolytic S was observed with high translational energies up to the allowed thermodynamic limit for gas phase *collinear* dissociation to ground state $S(^3P)$ and CO($J=0$). This indicates, for a significant part of the product, a major change in the geometry of the upper electronically excited $^1\Delta$ state from bent in the gas phase³¹ to

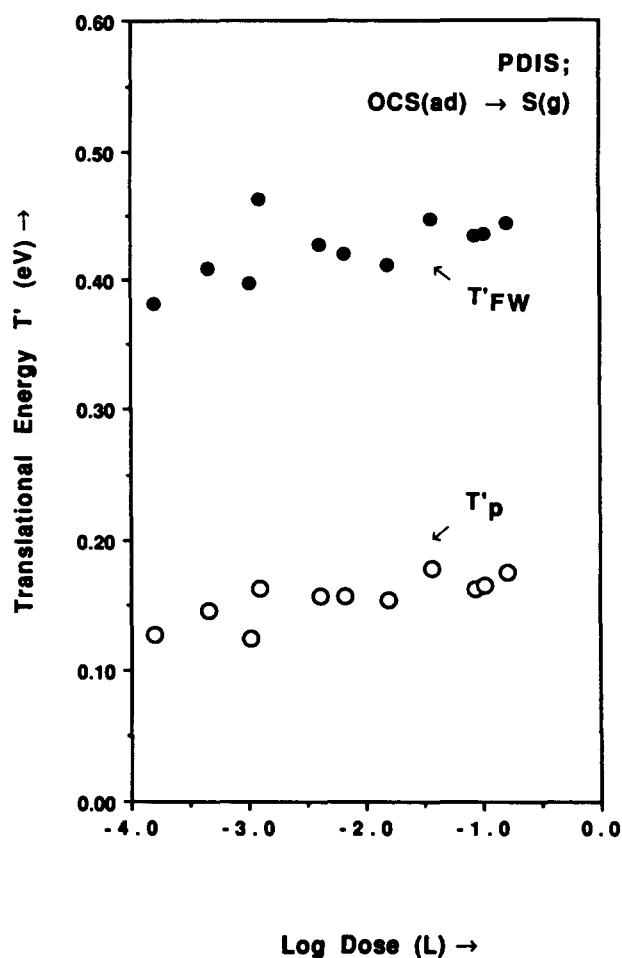


FIG. 6. Translational energy peak, T'_p , and FWHM, T'_{FW} , for the atomic sulphur fragment from 222 nm PDIS of OCS dose on unannealed LiF(001). The parameters of the energy distribution are only weakly dependent on adsorbate dose (and therefore surface site). Coverages were estimated to range from $\sim 10^{-4}$ ML to ~ 0.1 ML.

linear on LiF(001). Had the excited $^1\Delta$ state been similarly bent for OCS(ad), some of the energy available following photodissociation of the S-CO bond would have been deposited in CO rotation at the expense of translational energy in the S and CO fragments. Atomic sulphur product would then not be observed out to the allowed "thermodynamic" collinear translational energy limit. The S-CO bond dissociation energy inferred from the fastest sulphur fragments in TOF was consistent with best estimates of the bond dissociation energy, $D_0 = 3.12 \pm 0.03$ eV.⁴¹

The possible contribution of some *gas phase* photodissociation to the observed dynamics was assessed from the angular distribution of photolytic S. In the plane scanned by our detector, the angular distribution $P(\theta)$ of the photolytic sulphur was $\sim \cos \theta$ (θ = the polar angle to the surface normal); see Fig. 7.

The peaked $P(\theta)$ at $\theta = 0^\circ$ demonstrated that the photodissociation was occurring in the adsorbed state, since gas phase photolysis would yield an isotropic distribution of photofragments in the plane of detection for our unpolarized laser beam, as indicated in Fig. 7.

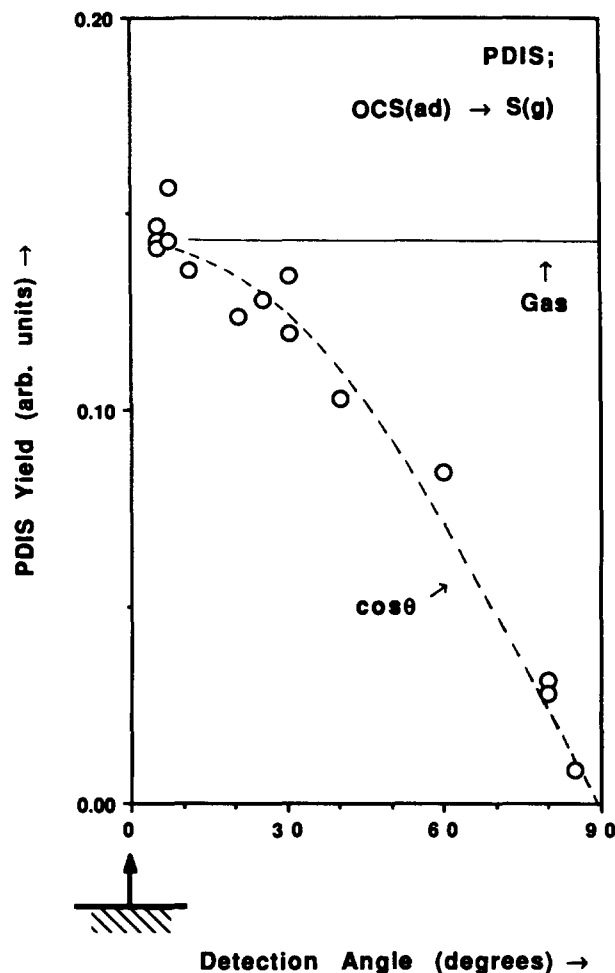


FIG. 7. Angular distribution $P(\theta)$ for the atomic sulphur photofragment from the 222 nm PDIS of OCS adsorbed on annealed LiF(001). The open symbols are the measured PDIS yields, while the dotted line is the fitted distribution ($\propto \cos \theta$ in this case). The surface normal (detection angle 0°) is sketched below the graph. The adsorbate coverage was 7×10^{-4} ML. Yields were measured to one "side" of the crystal normal. Distributions are symmetrical about the surface normal.

There remains the possibility that the observed dissociation product arises from gas phase photodissociation of photodesorbed OCS (see Ref. 6). If adsorbates were first promptly photodesorbed and then dissociated in the gas phase, they would travel a mean distance of ~ 30 wavelengths in a time of 6 ns (half the laser pulse duration). Averaging over desorbate orientation (the molecules now freely rotating in the gas) and the locally unpolarized laser field would again lead to an isotropic contribution to the PDIS angular distribution, in contrast to the observations of Fig. 7. The yield of dissociation fragments measured at a detection angle of 90° gives an upper limit on the contribution of gas phase dissociation to the total photolysis yield. As the yield of photodissociated molecules tended to zero as $\theta \rightarrow 90^\circ$, gas phase photolysis makes a negligible contribution to our results.

Further, the observation of photodissociation in the absence of molecular photodesorption (that would form a gas cloud) at very low adsorbate doses argues strongly

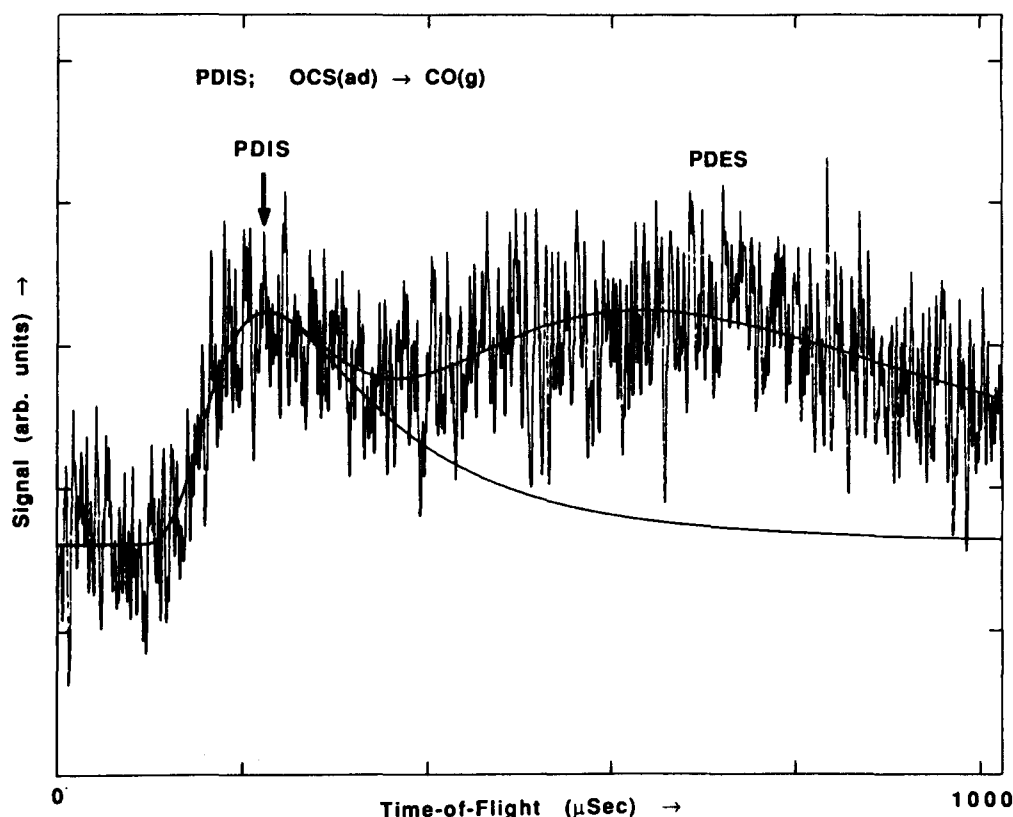


FIG. 8. Time-of-flight spectrum for the CO photofragment from the 222 nm PDIS of OCS physisorbed on annealed LiF(001) at 116 K. Daughter ion cracking product of the molecular PDES channel is also visible at later times. The spectrum was the signal averaged result of 6000 shots. The smooth curve is the least squares fit to the experimental data. The fit to the PDES channel is also shown. The surface coverage was estimated as 3.5×10^{-3} ML, with a laser energy of 8.6 mJ per laser pulse and a detection angle of 5° .

against photolysis of photodesorbates in the gas as the source of the observed photofragments.⁶

Finally, the observation of translational energy distributions $P(T')$ that differ markedly for OCS(g) and OCS(ad) is a telling argument against predominantly gas phase photodissociation.

The angular distribution of the photolysis product is believed to image the instantaneous orientation of OCS molecules on LiF(001). For an adsorbed OCS, the lifetime of the electronically excited state (gas phase $\tau_{\text{dis}} \sim 0.1$ ps)³¹ allows for a molecular rotation of only $\sim 6^\circ$ before dissociation occurs, based upon a rigid rotor model of OCS with a rotational temperature equal to the surface temperature.

The 308 nm photodissociation cross section enhancement at could not be determined, since no photodissociation product was detected when OCS(ad) was irradiated at 308 nm. The gas phase absorption cross section at 308 nm is decreased by five orders-of-magnitude⁴² from that at 222 nm. Had the adsorbed state 308 nm and 222 nm cross sections for photodissociation, $\sigma_{ph}(ad)$, been similarly enhanced (i.e. 10^3 – $10^4 \times$), the yield of PDIS fragments at 308 nm would still be below our detection limit.

B. CO photofragment

Figure 8 shows a TOF spectrum of the CO photofragment from the 222 nm photodissociation of OCS physisorbed on unannealed LiF(001). These data were collected at $\sim 3 \times$ the coverage of Fig. 1, owing to the residual gas pressure of CO always present in the UHV chamber.⁴³ The fitted distribution was transformed to give the translational energy distribution shown in Fig. 9 (b).

At an adsorbate coverage of 1×10^{-3} ML, the detected yields of S and CO photofragments were identical within

experimental error. This leads us to infer equal numbers of the two “vertical” orientations at low coverages. The relative numbers of the two orientations at high coverages could not be determined due to masking of the electron impact ionized PDIS signal in TOF by the daughter ion cracking products from the predominant PDES channel.

Figure 9(a) gives the translational energy distribution $P(T')$ for the gas phase photodissociation of OCS performed by Sivakumar *et al.*³¹ This distribution was again deduced from LIF measurements of the S and CO internal state distributions. As mirrored in the atomic sulphur photofragment energy distribution, the CO $P(T')$ had a bimodal appearance, the peaks being at 0.13 and 0.30 eV. The origin of this bimodality was the population of the CO fragments in rotational envelopes centered around $J=55$ and 66.

The adsorbed phase energy distribution is shown in Fig. 9(b). The peak energy was 0.08 eV and the T'_{FW} was 0.23 eV. This distribution corresponds to the photodissociation channel in the TOF spectrum of Fig. 8. The gas phase and adsorbed phase distributions are, once again, markedly different. As before, the adsorbed phase CO $P(T')$ showed no evidence of the bimodality present in gas phase photolysis. However, the peak translational energies of adsorbed and gas phase photolysis products were different: 0.08 versus 0.30 eV, respectively. The OCS(ad) CO peak translational energy, T'_p , appeared to correlate more closely with the CO($J=66$) channel of the gas phase distribution (0.08 versus 0.13 eV).

In contrast to the adsorbed phase $P(T')$ distribution for the sulphur fragment, the CO $P(T')$ distribution does not extend out to the expected “thermodynamic” limit for

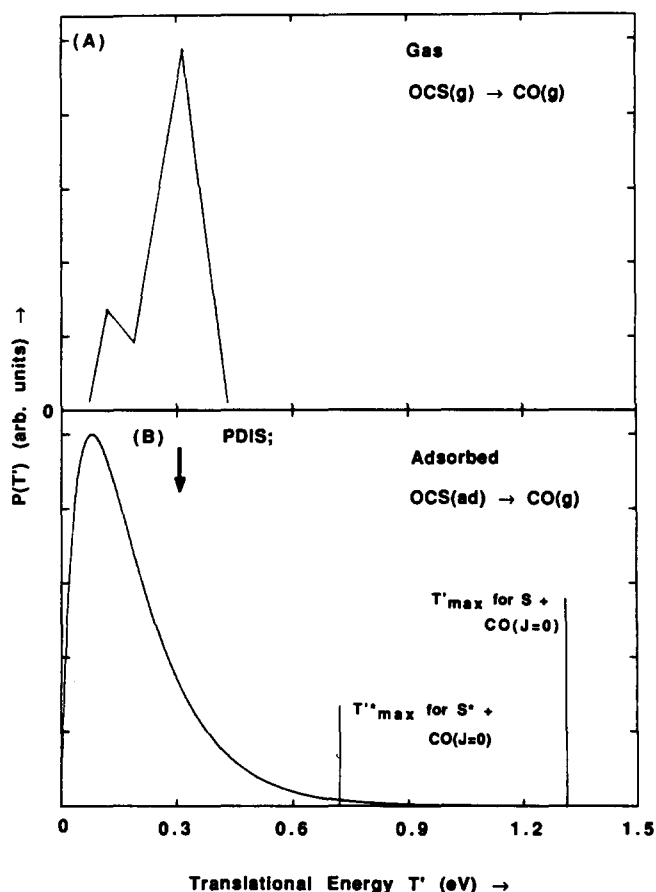


FIG. 9. Photofragment CO translational energy distribution $P(T')$ for the 222 nm photodissociation of OCS. (a) Gas phase distribution as inferred from the measured product state distribution of Sivakumar *et al.* (Ref. 31) (the bimodal structure reflects the population of two rotational components of the CO fragment energy distribution). (b) Adsorbed phase distribution as determined from the TOF spectrum of Fig. 8. The vertical arrow marks the peak of the gas phase translational energy distribution. The maximum "thermodynamic" translational energies for formation of ground state CO and atomic sulphur are also shown.

a collinear dissociation of 1.31 eV, but only extends to 0.9 eV. This discrepancy in energy probably arises from internal excitation, especially rotation, of the photolytic CO.

The most energetic S atoms were consistent with dissociation in a collinear $Su-OC-S$ ($Su = LiF$ surface) configuration. The most energetic CO (which had a translational energy well short of the thermodynamic limit), by contrast, implied dissociation through a bent $Su-S-CO$. These differing adsorbate geometries fit with the picture of energetic S recoiling directly into the gas at $\theta = 0^\circ$, and energetic CO recoiling from $Su-S-CO$.

C. Adsorbed state photodissociation cross section

The enhancement in photodissociation cross section for adsorbed OCS molecules, $\sigma_{ph}(ad)$, was established in three independent ways; (i)–(iii) below.

(i) First, for the previously studied system CH_3Br/LiF ,¹¹ the lowest dose for which photolysis products could be detected was $\sim 3 \times 10^{-3}$ L. Detailed calculations for that system on the number of photofragments indicated an adsorbed state photodissociation cross section

within a factor of two of the gas phase value of 2.3×10^{-19} cm²/mol.⁴⁴ By contrast, OCS photodissociation products could be detected for the remarkably low dose of $\sim 1 \times 10^{-5}$ L. The gas phase cross section for OCS is 1.1×10^{-19} cm²/mol;²⁷ one half that for CH_3Br . This suggested an adsorbed state cross section on the order of $10^3 \times$ the gas phase value.

(ii) Second, in all our previous studies of adsorbate photochemistry, the photolysis yield, PDIS, was less than the yield of molecular photodesorption, PDES.^{9–12} However, in the present instance, for adsorbate doses of less than 10^{-2} L/laser pulse, the integrated yield of photolysis products was greater than the photodesorbed product. In the limit of very low doses ($< 10^{-3}$ L), the photodesorption yield fell below detection limit, leaving only the photodissociation channel. The extent of adsorbate dissociation at low coverages was evaluated by comparison of PDIS and PDES yields at two wavelengths. At a coverage of 10^{-4} ML, the yield of PDIS (obtained at 222 nm, with no detectable PDES) was within a factor of two of the yield of PDES (obtained at 308 nm, where no photodissociation occurs). Therefore, it appears most likely that the absence of 222 nm PDES for low coverages is a result of complete photodissociation of the adsorbed layer: i.e. virtually all adsorbed molecules have been photodissociated.

As the number of photons incident on the crystal was 1×10^{15} cm⁻² (that is, 1 photon per 10 \AA^2), it follows that for complete photodissociation the photolytic cross section, $\sigma_{ph}(ad)$, must also have been on the order of 10 \AA^2 per molecule. This assumes a quantum efficiency for photodissociation of unity; for a smaller quantum efficiency $\sigma_{ph}(ad) > 10 \text{ \AA}^2/\text{mol}$. This estimate of the photolytic cross section is independent of the adsorbate coverage. To take an extreme example, even for an adsorbate "coverage" of 1 molecule, 1 photon per 10 \AA^2 leading to unit probability of photodissociation still implies $\sigma_{ph}(ad) \sim 10 \text{ \AA}^2$ per molecule.

(iii) A third approach to the estimate of $\sigma_{ph}(ad)$ involves detailed calculation of the cross section from considerations of the radiation absorbed, the adsorbate coverage and the observed yield of photofragments. The attenuation of radiation by absorption in a sample of gas is given by Beer's Law:

$$I_f = I_o [1 - \exp(-N\sigma_{ph})]$$

where I_o and I_f are the incident and final intensities, N is the number of absorbers and σ_{ph} is the absorption cross section. For an adsorbate, the yield of photodissociation product can be given by:

$$N_{dis} = A\zeta I_o [1 - \exp(-SD\sigma_{ph}(ad))] \Phi,$$

where N_{dis} is the number of dissociated absorbers, A the surface area illuminated and ζ the attenuation of the laser field by destructive interference between incident and reflected radiation. N has been replaced by the product of the sticking probability S and the adsorbate dose D in molecules per unit area. The absorption cross section now applies to the adsorbed state: $\sigma_{ph}(ad)$. The term Φ accounts for the quantum efficiency of photodissociation once a photon has been absorbed.

Recasting the formula in terms of experimental parameters, I_o is replaced by $kF_o/h\nu$, where F_o is the incident laser energy in mJ per laser pulse and $h\nu$ is the photon energy. As the LiF crystal face does not intercept the entire laser beam, k allows for this reduction in the number of incident photons (for this apparatus, $k=0.38$). For a monolayer coverage, SD is on the order of 10^{14} – 10^{15} cm^{-2} . Absorption cross sections for gases in the ultraviolet are usually much less than 10^{-15} cm^2 . As the product of $SD\sigma_{ph}(ad)$ is much less than 1, the exponential term can be expanded and simplified to give:

$$N_{dis} = A\xi SD \times \sigma_{ph}(ad) \times \Phi kF_o/h\nu. \quad (1)$$

Equation (1) describes the relationship between the observed photoproduct yield and the product of the cross section for photodissociation in the adsorbed state and the quantum efficiency for photodissociation. As we had no independent method to determine Φ , it was assumed equal to one. This gave a lower limit for the adsorbed state photolytic cross section $\sigma_{ph}(ad)$; significant quenching would imply a larger cross section than we report.

The following exemplifies our findings using Eq. 1. The photolytic cross section for the TOF of Fig. 1 was calculated as $\sigma_{ph}(ad) = 8.5 \times 10^{-17}$ cm^2/mol ($0.85 \text{ \AA}^2/\text{mol}$). This adsorbed state photolytic cross section is $\sim 780\times$ the gas phase value. Hence for low coverages of $\text{OCS}(ad)$ on LiF(001), $\sigma_{ph}(ad) \sim 1$ – 10 \AA^2 per molecule, in agreement with estimates by the two more approximate methods given above.

At an adsorbate dose of 4.2×10^{-3} L on annealed LiF(001), the photolytic cross section enhancement calculated from the observed CO yield was equal, within a factor of $2\times$, to that obtained for the atomic sulphur fragment under similar conditions. The yield of PDIS was consistent with virtually complete photodissociation of the adsorbate layer. For these conditions, the analysis used here provides only lower limits to the adsorbed state photolytic cross section $\sigma_{ph}(ad)$; the smallest laser exposure (in photons per cm^2) at which complete PDIS occurs was not measured. Therefore, the number of photons necessary for complete PDIS could be overestimated and $\sigma_{ph}(ad)$ underestimated.

For higher adsorbate coverages where some PDES was also detected, the photodissociation of the adsorbed layer was now clearly incomplete. For these conditions, a linear relation between laser energy and PDIS yield applied [Eq. (1)].

D. Mechanism of adsorbed state photodissociation

An apparent orders-of-magnitude increase in photofragment yield from $\text{OCS}(ad)$ as compared with that obtained for $\text{OCS}(g)$ could in principle be due to the fact that the adsorbate coverage accumulated, being orders-of-magnitude higher than the adsorbate dose. This was, however, disproved in three ways.

First, for the lowest adsorbate doses ($\sim 10^{-5}$ L/laser pulse) even assuming unit sticking probability, the duration of the experiment was insufficient for the surface (initially clean) to accumulate sufficient coverage to account

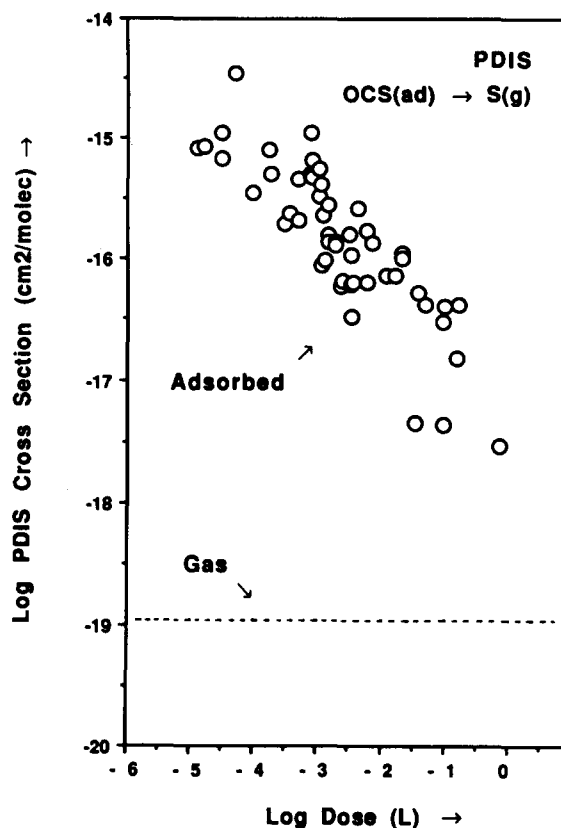


FIG. 10. Adsorbed state photodissociation cross section $\sigma_{ph}(ad)$ as a function of OCS dose. These data were collected from several crystals cleaved from different boules, with varying heat treatments and degrees of surface contamination. The extent of the variation in PDIS cross section at a given coverage amounts to an order of magnitude in $\sigma_{ph}(ad)$.

for the observed photofragment yield, assuming the gas phase photolytic cross section $\sigma_{ph}(g)$. This calculation neglected concurrent removal of adsorbate by any (photolytic or nonphotolytic) process; including this factor makes the supposed high coverage still less credible. Second, the experimental yields were stable with respect to experiment time: Experiments comprising N or $2N$ laser pulses gave identical yields of photofragments. The “accumulation” model would predict different yields. Finally, experimental yields were independent of “memory effects”; for experiments done in the sequence “high” dose then “low” dose, the yields decreased for the second experiment. Again, the model that assumes an accumulation of dosed material would predict comparable yields for the two experiments.

We conclude that we have observed a real increase in $\sigma_{ph}(ad)$ of 10^3 – $10^4\times$ as compared with $\sigma_{ph}(g)$.

The sensitivity of the cross section enhancement to variations in the substrate amounted to an order of magnitude (Fig. 10). These variations included contributions from crystals cleaved from different LiF boules, from detection angles other than normal incidence, degrees of sulphur and carbon surface deposits and heat treatment. The enhancement was not a strong function of surface deposits. Therefore, the differences between crystals cleaved from different LiF boules suggest bulk or surface defects.

The sensitivity of the enhancement to crystal heat treatment is illustrated in Fig. 11. Following annealing of

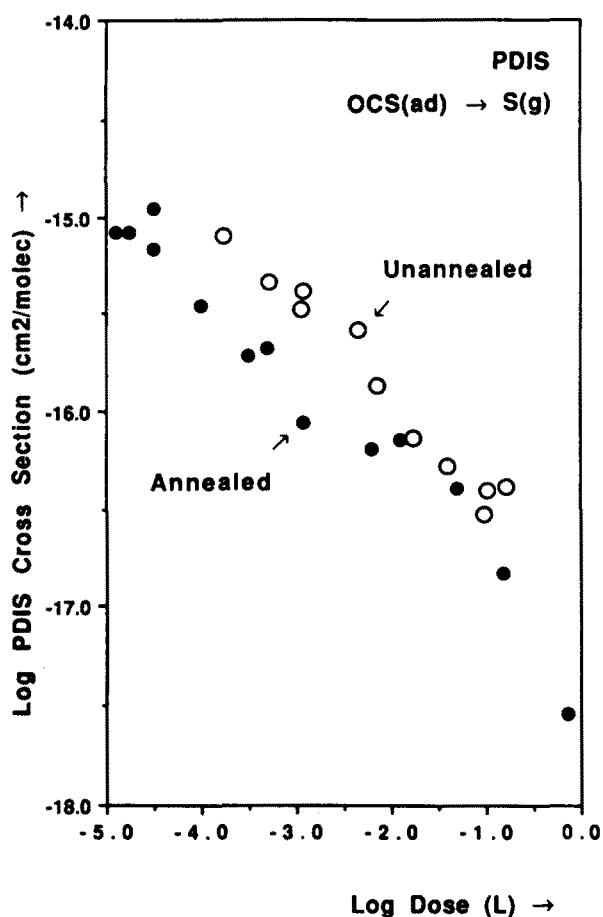


FIG. 11. Sensitivity of the adsorbed state photolytic cross section $\sigma_{ph}(ad)$ to crystal heat treatment. The cross section is $0.1 \times$ as great on the annealed crystal at doses $< 10^{-2}$ L. The annealed and unannealed curves converge for doses $> 10^{-2}$ L.

the crystal, $\sigma_{ph}(ad)$ for a given coverage ($< 10^{-2}$ ML) decreased by an order of magnitude. This would be expected if heat treatment (i.e. annealing) reduced the number of "active sites" responsible for the enhancement. That the cross section enhancement was greatest at low coverages suggested that surface defects are important. The sensitivity of the enhancement to heat treatment further suggests the involvement of bulk or surface defects.

Among the possible candidates for defects are F -centers. The F -center absorption band of LiF encompasses both the KrCl and XeCl excimer wavelengths used in this study.⁴⁵ Stokes-shifted radiation characteristic of F -center de-excitation was observed from the laser-irradiated crystal employed in these experiments.⁴⁶ Defect F -center concentrations commonly reported for alkali halide crystals are on the order of 10^{16} cm^{-3} (equivalently $\sim 10^{-4}$ ML on a surface).⁴⁷ As the enhanced PDIS cross sections could be observed up to coverages ~ 0.2 ML, this implied an effect not solely due to adsorption in proximity to a surface F -center, perhaps involving F -centers in the crystal bulk.

Proximity of the OCS to the LiF surface was necessary for the enhancement effect. Interposing an "ice" of H_2O between the OCS and the LiF was found to reduce the photodissociation yield to below detection limit. This marked decrease of photolysis yield implied a decreased

cross section enhancement due to the separation of the $\text{OCS}(ad)$ from the LiF surface. Such a decline in $\sigma_{ph}(ad)$ is consistent with the other evidence for the importance of defect sites at and near the LiF surface in giving rise to the enhanced $\sigma_{ph}(ad)$.

In the following paragraphs we consider several mechanisms that might account for the observed large increase in $\sigma_{ph}(ad)$ relative to $\sigma_{ph}(g)$.

(1) Adsorption on LiF could reduce the symmetry of the OCS molecule from $C_{\infty v}$ to C_s . The optical transition would then become electric dipole allowed, with a corresponding increase in photolytic cross section. However, even a fully allowed transition in this wavelength region would have $\sigma_{ph}(g)$ only on the order of 10^{-18} to $10^{-17} \text{ cm}^2/\text{mol}$. Enhanced UV absorption coefficients for molecules in the adsorbed state relative to the gas phase have been reported for several systems, including dimethylcadmium on fused silica,⁷ solid OCS at 53 K,⁴⁸ and $\text{Fe}(\text{CO})_5$ on Si(111).⁴⁹ However, these enhancement factors only varied over the range from 4.4 up to 12, reflecting in part spectral shifts upon adsorption.⁷ In connection with this model it may also be worth noting that if a substantial fraction of OCS has its symmetry in the adsorbed state reduced from $C_{\infty v}$ to C_s , i.e. from linear to bent, then as the photodissociation occurred, torque would be imparted to the CO fragment, resulting in some degree of rotational excitation. Consequently photolytic S would not be observed out to the allowed thermodynamic limit for a collisional dissociation, as is found to be the case.

(2) If adsorption in the neighborhood of a surface defect site brought about a change in the molecular geometry (comparable to vibrational excitation), then the adsorbed state dissociation cross section could exhibit an enhancement relative to the gas phase. In the case of $\text{OCS}(g)$, excitation of $2\nu_2$ has been shown to lead to a dissociation enhancement relative to the ground vibrational state of $\sim 20 \times$.⁵⁰ Selwyn and Johnston have reported similar absorption cross section enhancements, on the order of $4.5 \times$, for excitation of the ν_2 mode of N_2O in the A-X band.⁵⁰ It would appear necessary to postulate a surprisingly large distortion of $\text{OCS}(ad)$ upon physisorption in order to account for the three to four orders-of-magnitude increase in σ_{ph} that we observe. It is not known whether there exists any distortion that could result in such a large change in σ_{ph} .

(3) Enhanced Raman scattering cross sections ($\sim 10^5$ – $10^6 \times$) have been detected for a variety of molecules adsorbed on roughened metal surfaces, including lithium.² The dominant mechanism leading to surface enhanced Raman scattering (SERS) is the electric field enhancement in the vicinity of small metallic features. On resonance or near resonance with the external laser field, the surface plasmons of small roughness features lead to an increased effective field at the particle surface.²

It is possible that a small quantity of metallic lithium as a surface impurity on the LiF could lead to a SERS-like enhancement in intensity. These lithium adatoms could form in clusters, though the sizes would be much smaller than the $> 100 \text{ \AA}$ diameter features typically observed

from silver surfaces.² Moreover, the observation of substantial enhancements for coverages approaching 0.1 ML and larger, implied a mechanism not restricted exclusively to a small subset of surface sites.

(4) An alternative mechanism for the enhancement in the photodissociation cross section would involve photoinduced charge transfer from the substrate to the adsorbate. The dissociative electron attachment cross section for $\text{OCS} + e^- \rightarrow \text{S}^- + \text{CO}$ has been measured in the gas phase; $\sigma_e \sim 0.1 \text{ \AA}^2/\text{mol}$ (Ref. 51) (cf. 1–10 \AA^2 per molecule for surface-enhanced photodissociation). The phenomenon of enhanced photoconductivity of LiF under UV irradiation has been well established,⁴⁵ and could serve as the source of the electrons. Once in the conduction band, these delocalized electrons can move to defects at the surface or adsorbates. Trapping of some photoelectrons in vacancies at or near the surface could result in a higher local density of electron-rich defects adjacent to the adsorbate.

However, it is unlikely that these electrons could induce dissociative attachment in OCS since the peak cross section for dissociative attachment in the gas phase is $\sim 1 \text{ eV}$.⁵¹ The thermalized photoelectrons would have a peak energy $\sim 1 \text{ meV}$ (at 115 K), an energy for which there is negligible dissociative attachment cross section. Therefore dissociative attachment in $\text{OCS}(ad)$ is unlikely to be initiated efficiently by electrons generated photolytically from LiF.

The observation of similar yields of S and CO *neutrals* in this work also argues against $\text{OCS} + e^- \rightarrow \text{S}^- + \text{CO}$. Our mass spectrometer is not configured for negative ion detection. Only if the departing S^- returns its electron to the surface would the yields of neutral S equal neutral CO. Temporary negative ion formation following molecule-metal surface collisions has been proposed for some systems, analogous to that observed in gas phase inelastic electron scattering.⁵² However, such long range charge transfer appears improbable in the present case of a dielectric substrate; it would have to occur with almost unit probability for this charge-transfer mechanism to apply.

(5) A further model for the observed enhancement in σ_{ph} would make use of *F*-centers in the crystal as an extended absorber of UV and as a source of electron energy in electronic-to-electronic (*E*→*E*) transfer. This *E*→*E* energy transfer could occur from *F*-centers in the region of the surface to the adsorbed OCS molecule. Strong coupling between the excited state of *F*-centers and OH^- defects has been observed in KCl crystals.⁵³ The coupling occurs for low defect concentrations, over long ranges, $\sim 300 \text{ \AA}$,⁵⁴ so that *F*-centers below the surface could contribute to the energy transfer.

Moreover, there is evidence for mobility of *F*-centers in LiF.⁴⁷ The illuminated bulk LiF would then also serve as a collector of the incident energy. Hence, the efficiency of conversion of the incident energy into dissociation products would be high as compared with that in the absence of substrate. In effect, the substrate would become an antenna for collecting photons. The measured timescale for this energy transfer was rapid;⁵³ $\sim 100 \text{ ps}$ for the analogous

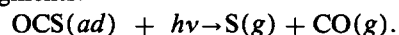
F-center to OH^- *E*→*E* transfer. It follows that a single *F*-center could be involved in many *E*→*E* energy transfers during the $\sim 10^{-8} \text{ s}$ duration of the laser illumination.

To assess the possible role of surface *F*-centers in the observed enhancement, photolysis experiments were performed concurrently with electron beam irradiation (400 eV, 3 μA total current broadly directed toward the crystal for 30 min). Production of *F*-centers under electron beam irradiation has been observed in LiF.⁵⁵ No significant change in $\sigma_{ph}(ad)$ was detected. This would be understandable if energy transfer from *F*-centers within the bulk of the crystal made the major contribution to $\sigma_{ph}(ad)$.

Of the possible enhancement mechanisms described above, we favor the long range *F*-center mediated *E*→*E* transfer (#5) or perhaps the dissociative electron attachment mechanism (#4).

IV. CONCLUSIONS

The 222 nm photodissociation of OCS physisorbed on LiF(001) was investigated by angle-resolved TOF mass spectrometry of both the atomic sulphur and CO photo-fragments:



For low coverages ($\sim 10^{-4} \text{ ML}$), the 222 nm cross section for photodissociation in the adsorbed state, $\sigma_{ph}(ad)$, was found to be enhanced by 10^3 – $10^4 \times$ relative to the gas phase, and was a decreasing function of increasing adsorbate dose, and hence coverage. Annealed LiF was $\sim 0.1 \times$ as effective in catalyzing photodissociation as was unannealed LiF. Only an upper limit of $\leq 10^3 \times$ could be set on the enhancement in the absorption cross section at 308 nm.

At 222 nm, photolytic sulphur was observed with translational energies up to the thermodynamic limit for a collinear gas phase dissociation, suggestive of an altered upper excited state geometry for some of the dissociation product. The translational energy distribution $P(T')$ of the sulphur fragment showed no evidence of the bimodality present in gas phase photodissociation. The $P(T')$ distribution was weakly dependent on adsorbate coverage and crystal surface. The photolytic branching ratio, $R = (\text{S}^*/\text{S})$, between excited state and ground state sulphur shifted from ∞ in the gas phase to an upper limit of 3 in the adsorbed state. The peak translational energy for $\text{OCS}(ad) + h\nu \rightarrow \text{S}(g)$ for a coverage of $\sim 0.1 \text{ ML}$ was $T'_p = 0.24 \text{ eV}$ with a FWHM, T'_{FW} , of 0.54 eV. The corresponding quantities for gaseous photodissociation are $T'_p = 0.27 \text{ eV}$ and $T'_{FW} = 0.12 \text{ eV}$.

These changes in the magnitude of $\sigma_{ph}(ad)$, the branching ratio R , and the translational energy distribution as compared with the corresponding quantities for the gas phase were indicative of markedly altered dissociation dynamics in the adsorbed state.

For low adsorbate coverages of $< 10^{-3} \text{ ML}$ and modest laser energies of $\sim 8 \text{ mJ/laser pulse}$, the extent of dissociation of the adsorbed OCS layer appears to be complete; virtually all adsorbed molecules are photodissociated.

The angular distribution $P(\theta)$ of the sulphur photo-fragment was peaked around the surface normal ($\sim \cos \theta$), representing the average orientation of OCS on LiF(001) at 116 K. This angular distribution was invariant over the coverage range 10^{-4} to ~ 0.1 ML.

The CO translational energy distribution for $\text{OCS}(ad) + hv \rightarrow \text{CO}(g)$ did not extend to the "thermodynamic" limit for collinear dissociation. Internal excitation of the CO is the most probable sink for this missing energy. The peak translational energy was $T'_p = 0.08$ eV with a FWHM, T'_{FW} , of 0.24 eV as compared with $T'_p = 0.30$ eV and $T'_{FW} = 0.13$ eV for gaseous photodissociation. The 222 nm cross section for photodissociation leading to photo-fragment CO was enhanced (as in the case of the sulphur photo-fragment) by $\sim 10^3 \times$ relative to the gas phase value; i.e. the yields of sulphur and CO fragments were comparable.

The observations of greatly enhanced adsorbate photodissociation cross section were indicative of a catalytic influence of the LiF crystal. This "photocatalysis" may originate in efficient $E \rightarrow E$ electronic energy transfer from LiF defect sites (F -centers) to the adsorbate. Excited F -centers within a "skin depth" of the surface corresponding to hundreds of Å could transfer their excitation to the adsorbed OCS, leading to dissociation with high efficiency; in this case the substrate constitutes an antenna for collecting photons that give rise to photodissociation. Other possible contributing factors are discussed.

ACKNOWLEDGMENTS

St. J. Dixon-Warren and M. S. Matyjaszczyk are thanked for assistance with experiments. Helpful discussions with Prof. D. J. Donaldson are gratefully acknowledged. This work was made possible through the generous support of the University of Toronto, the Natural Sciences and Engineering Research Council of Canada, the Venture Research Unit (BP Canadian Holdings, Ltd.), and the Ontario Laser and Lightwave Research Centre.

- ¹ See for example: R. M. Osgood, *Ann. Rev. Phys. Chem.* **34**, 77 (1983); T. J. Chuang, *Surf. Sci. Rep.* **3**, 1 (1983); J. Lin, W. C. Murphy, and T. F. George, *Ind. Eng. Chem. Prod. Res. Dev.* **23**, 334 (1984); *Laser Controlled Chemical Processing of Surfaces*, edited by A. W. Johnson, D. J. Ehrlich, and H. R. Sclossberg (Elsevier, New York, 1985); T. J. Chuang, *Surf. Sci.* **178**, 763 (1986).
- ² M. Moskovits, *Rev. Mod. Phys.* **57**, 783 (1985); *J. Chem. Phys.* **69**, 4159 (1978); also A. Campion, *Ann. Rev. Phys. Chem.* **36**, 549 (1985).
- ³ St. J. Dixon-Warren, I. Harrison, K. Leggett, M. S. Matyjaszczyk, J. C. Polanyi, and P. A. Young, *J. Chem. Phys.* **88**, 4092 (1988).
- ⁴ P. A. Young, Ph.D. Thesis, University of Toronto, 1989.
- ⁵ St. J. Dixon-Warren, K. Leggett, M. S. Matyjaszczyk, J. C. Polanyi, and P. A. Young, *J. Chem. Phys.* **93**, 3659 (1990).
- ⁶ J. C. Polanyi and P. A. Young, *J. Chem. Phys.* **93**, 3673 (1990).
- ⁷ C. J. Chen and R. M. Osgood, *Phys. Rev. Lett.* **50**, 1705 (1983); *Appl. Phys.* **A31**, 171 (1982).
- ⁸ J. Y. Tsao and D. J. Ehrlich, *J. Chem. Phys.* **81**, 4620 (1984).
- ⁹ E. B. D. Bourdon, J. P. Cowin, I. Harrison, J. C. Polanyi, J. Segner, C. D. Stanners, and P. A. Young, *J. Phys. Chem.* **88**, 6100 (1984).
- ¹⁰ E. B. D. Bourdon, P. Das, I. Harrison, J. C. Polanyi, J. Segner, C. D. Stanners, R. J. Williams, and P. A. Young, *Faraday Discuss. Chem. Soc.* **82**, 343 (1986).
- ¹¹ I. Harrison, J. C. Polanyi, and P. A. Young, *J. Chem. Phys.* **89**, 1475 (1988).
- ¹² I. Harrison, J. C. Polanyi, and P. A. Young, *J. Chem. Phys.* **89**, 1498 (1988).
- ¹³ F. L. Tabares, E. P. Marsh, G. A. Bach, and J. P. Cowin, *J. Chem. Phys.* **86**, 738 (1987).
- ¹⁴ N. Nishi, H. Shinohara, and T. Okuyama, *J. Chem. Phys.* **80**, 3898 (1984).
- ¹⁵ N. Nishi, *Faraday Discuss. Chem. Soc.* **82**, 384 (1986).
- ¹⁶ J. Kutzner, G. Lindeke, K. H. Welge, and D. Feldmann, *J. Chem. Phys.* **90**, 548 (1989).
- ¹⁷ K. Domen and T. J. Chuang, *Phys. Rev. Lett.* **59**, 1484 (1987).
- ¹⁸ K. Domen and T. J. Chuang, *J. Chem. Phys.* **90**, 3318 (1989).
- ¹⁹ K. Domen and T. J. Chuang, *J. Chem. Phys.* **90**, 3338 (1989).
- ²⁰ J. S. Foord and R. B. Jackman, *Chem. Phys. Lett.* **112**, 190 (1984); J. R. Swanson, C. M. Friend, and Y. J. Chabal, *J. Chem. Phys.* **87**, 5028 (1987); C. E. Bartosch, N. S. Gluck, W. Ho, and Z. Ying, *Phys. Rev. Lett.* **57**, 1425 (1986); and J. R. Swanson and C. M. Friend, *J. Vac. Sci. Technol. A* **6**, 770 (1988).
- ²¹ S. A. Costello, B. Roop, Z.-M. Liu, and J. M. White, *J. Phys. Chem.* **92**, 1019 (1988); E. P. Marsh, T. L. Gilton, W. Meier, M. R. Schneider, and J. P. Cowin, *Phys. Rev. Lett.* **61**, 2725 (1988).
- ²² G. S. Higashi, *J. Chem. Phys.* **88**, 422 (1988).
- ²³ I. Harrison and J. C. Polanyi, *Z. Phys. D* **10**, 383 (1988).
- ²⁴ J. W. Rabalais, J. M. Macdonald, V. Scherr, and S. P. McGlynn, *Chem. Rev.* **71**, 73 (1971).
- ²⁵ K. Sidhu, I. G. Csizmadia, O. P. Strausz, and H. E. Gunning, *J. Am. Chem. Soc.* **88**, 2412 (1966).
- ²⁶ W. H. Breckenridge and H. Taube, *J. Chem. Phys.* **52**, 1713 (1970) and B. M. Ferro and B. G. Reuben, *Trans. Faraday Soc.* **67**, 2847 (1971).
- ²⁷ H. Okabe, *Photochemistry of Small Molecules* (Wiley-Interscience, New York, 1978), p. 215.
- ²⁸ W. Lochte-Holtgreven, C. E. H. Bawn, and E. Eastwood, *Nature* **129**, 869 (1932).
- ²⁹ A. R. Knight, O. P. Strausz, S. M. Malm, and H. E. Gunning, *J. Am. Chem. Soc.* **86**, 4243 (1964); H. E. Gunning and O. P. Strausz, *Adv. Photochem.* **4**, 133 (1966); W. H. Breckenridge and H. Taube, *J. Chem. Phys.* **53**, 1750 (1970).
- ³⁰ J. A. Joens and E. J. Bair, *J. Phys. Chem.* **88**, 6009 (1984).
- ³¹ N. Sivakumar, G. E. Hall, P. L. Houston, J. W. Hepburn, and I. Burak, *J. Chem. Phys.* **88**, 3692 (1988); N. Sivakumar, I. Burak, W.-Y. Cheung, P. L. Houston and J. W. Hepburn, *J. Phys. Chem.* **89**, 3609 (1985); and P. L. Houston (private communication).
- ³² G. Roy, G. Singh, and T. E. Gallon, *Surf. Sci.* **152**, 1042 (1985); J. Estel, H. Hoinkes, H. Kaarman, H. Nahr, and H. Wilsch, *Surf. Sci.* **54**, 393 (1976) and D. G. Lord and T. E. Gallon, *Surf. Sci.* **36**, 606 (1973).
- ³³ W. Braker and A. L. Mossman, *Matheson Gas Data Book, 5th ed.*, (Matheson Gas Products, New Jersey, 1971), p. 115.
- ³⁴ S. Dushman and A. H. Young, *Phys. Rev.* **68**, 278 (1945) and S. Wagener and C. B. Johnson, *J. Sci. Inst.* **18**, 278 (1951).
- ³⁵ P. D. Townsend and J. C. Kelly, *Phys. Lett.* **26A**, 138 (1968) and P. W. Palmberg and T. N. Rhodin, *J. Phys. Chem. Solids* **29**, 1917 (1968).
- ³⁶ Harshaw Optical Crystal Catalog, Harshaw Chemical Co., 6801 Cochran Rd., Solon, Ohio, 44139.
- ³⁷ H. H. Landolt and R. Bornstein, *Zahlenwerte und Funktionen, 6th ed., Vol. 2, Part IV* (Springer, Berlin, 1961), p. 418.
- ³⁸ Taken from the density of OCS(*s*). See: L. Vegard, *Z. Krist.* **77**, 411 (1931).
- ³⁹ G. Comsa and R. David, *Surf. Sci. Rep.* **5**, 145 (1985).
- ⁴⁰ Direct excitation of Xe by two photon absorption of 248 nm radiation has been reported for KrF laser powers of 3000 MW/cm². See: D. Klinger, D. Pritchard, W. K. Bischel, and C. K. Rhodes, *J. Appl. Phys.* **49**, 2219 (1978).
- ⁴¹ D. R. Stull and H. Prophet, *JANAF Thermochemical Tables, 2nd ed.*, Nat. Stand. Ref. Data Serv., Nat. Bur. Stand. (US) **37**, 1971.
- ⁴² L. T. Molina, J. J. Lamb, and M. J. Molina, *Geophys. Res. Lett.* **8**, 1008 (1981).
- ⁴³ W. M. Brubaker in *Methods of Experimental Physics, Volume 14: Vacuum Physics and Technology*, edited by G. L. Weissler and R. W. Carlson (Academic, New York, 1979), p. 99.
- ⁴⁴ H. Okabe, *Photochemistry of Small Molecules* (Wiley-Interscience, New York, 1978), p. 300.
- ⁴⁵ R. K. Swank and F. C. Brown, *Phys. Rev.* **130**, 34 (1963).
- ⁴⁶ W. B. Fowler in *Physics of Colour Centres*, edited by W. B. Fowler (Academic, New York, 1968), Ch. 2.
- ⁴⁷ See for example: G. M. Loubriel, T. A. Green, P. M. Richards, R. G.

- Albridge, D. W. Cherry, R. K. Cole, R. F. Haglund Jr., L. T. Hudson, M. H. Mendenhall, D. M. Newns, P. M. Savundararaj, K. J. Snowdon, and N. H. Tolk, *Phys. Rev. Lett.* **57**, 1781 (1986) and K. Park, *Phys. Rev.* **140**, A1735 (1965).
- ⁴⁸K. M. Monahan and W. C. Walker, *J. Chem. Phys.* **63**, 5126 (1975).
- ⁴⁹J. R. Swanson, C. M. Friend, and Y. J. Chabal, *J. Chem. Phys.* **87**, 5028 (1987).
- ⁵⁰P. F. Zittel and D. E. Masturzo, *J. Chem. Phys.* **85**, 4362 (1986); G. S. Selwyn and H. S. Johnston, *J. Chem. Phys.* **74**, 3791 (1981).
- ⁵¹J. P. Ziesel, G. J. Schulz, and J. Milhaud, *J. Chem. Phys.* **62**, 1936 (1975); K. A. G. McNeil and J. C. J. Thynne, *J. Phys. Chem.* **73**, 2960 (1969); and M. J. Hubin-Franskin, J. Katihabwa, and J. E. Collin, *Int. J. Mass. Spec. Ion. Phys.* **20**, 285 (1976).
- ⁵²J. W. Gadzuk, *J. Chem. Phys.* **79**, 6341 (1983) and T. M. Stephen Xueying Shi, and P. D. Barrow, *J. Phys. B* **21**, L169 (1988).
- ⁵³D.-J. Jang, T. C. Corcoran, M. A. El-Sayed, L. Gomes, and F. Luty in *Ultrafast Phenomena V*, edited by G. R. Fleming and A. E. Siegman (Springer, Berlin, 1986), p. 280.
- ⁵⁴M. A. El-Sayed (private communication).
- ⁵⁵D. G. Lord, *Phys. Stat. Sol. B* **43**, K115 (1971) and K. Toriumi and N. Itoh, *Phys. Stat. Sol. B* **107**, 375 (1981).